The PtAl and PtAl2 anions: Theoretical and photoelectron spectroscopic characterization

Xinxing Zhang, Gerd Ganteför, Kit H. Bowen, and Anastassia N. Alexandrova

Citation: The Journal of Chemical Physics **140**, 164316 (2014); doi: 10.1063/1.4873160
View online: http://dx.doi.org/10.1063/1.4873160
View Table of Contents: http://scitation.aip.org/content/aip/journal/jcp/140/16?ver=pdfcov
Published by the AIP Publishing

Articles you may be interested in

Photoelectron spectroscopy and theoretical studies of UF5 and UF6
J. Chem. Phys. **136**, 194304 (2012); 10.1063/1.4716182

Valence isoelectronic substitution in the B8 and B9 molecular wheels by an Al dopant atom: Umbrella-like structures of AlB7 and AlB8
J. Chem. Phys. **135**, 104301 (2011); 10.1063/1.3625959

Spectroscopic properties of novel aromatic metal clusters: NaM 4 (M = Al,Ga,In) and their cations and anions
J. Chem. Phys. **120**, 10501 (2004); 10.1063/1.1738112

Geometries and spectroscopic properties of germanium and tin hexamers (Ge 6 ,Ge 6 + ,Ge 6 ,Sn 6 ,Sn 6 + , and Sn 6)
J. Chem. Phys. **115**, 3121 (2001); 10.1063/1.1386795

A study of the structure and bonding of small aluminum oxide clusters by photoelectron spectroscopy: Al x O y (x=1–2, y=1–5)
J. Chem. Phys. **106**, 1309 (1997); 10.1063/1.474085

This article is copyrighted as indicated in the article. Reuse of AIP content is subject to the terms at: http://scitation.aip.org/termsconditions. Downloaded to IP: 128.220.159.3 On: Wed, 30 Apr 2014 18:26:58

The $PtAl^-$ and $PtAl_2^-$ anions: Theoretical and photoelectron spectroscopic characterization

Xinxing Zhang,[1] Gerd Ganteför,[1] Kit H. Bowen,[1,a)] and Anastassia N. Alexandrova[2,a)]
[1]*Departments of Chemistry and Materials Science, Johns Hopkins University, Baltimore, Maryland 21218, USA*
[2]*Department of Chemistry and Biochemistry, University of California, Los Angeles, Los Angeles, California 90095-1569, USA and California NanoSystems Institute, 570 Westwood Plaza, Building 114, Los Angeles, California 90095, USA*

(Received 21 January 2014; accepted 14 April 2014; published online 30 April 2014)

We report a joint photoelectron spectroscopic and theoretical study of the $PtAl^-$ and $PtAl_2^-$ anions. The ground state structures and electronic configurations of these species were identified to be $C_{\infty v}$, $^1\Sigma^+$ for $PtAl^-$, and C_{2v}, $^2B_1$ for $PtAl_2^-$. Structured anion photoelectron spectra of these clusters were recorded and interpreted using *ab initio* calculations. Good agreement between theory and experiment was found. All experimental features were successfully assigned to one-electron transitions from the ground state of the anions to the ground or excited states of the corresponding neutral species. © *2014 AIP Publishing LLC*. [http://dx.doi.org/10.1063/1.4873160]

INTRODUCTION

Small bimetallic clusters containing precious metal elements are of great interest in catalysis (see, for example, Refs. 1–8). Indeed, doping is being explored as one of the most promising means of tuning the catalytic activity of clusters and nanoparticles of Pt, Pd, and Au, although often in an empirical way. To understand the catalysis mechanism of these binary metallic clusters, to explore the reason why they are better than single element clusters, and to know how their properties depend so radically on their size and composition, determining their electronic structures, and realizing how they change with doping are the first steps. These types of studies, however, are scarce. It is purported that doping the second metal can be used to tune the electronic structures by adjusting the position of the d-band center.[4] Çakır and Gülseren studied the electronic structures of TiO_2 supported Pt_2Au_m (m = 1–5) clusters, and found that the presence of the Pt dimer remarkably enhances the binding energy and limits the migration of Au atoms on the titania surface.[5] A first-principle study of CO oxidation catalyzed by TiO_2 supported Pd_4Au and Pd_5 clusters showed that the bimetallic Pd_4Au has enhanced catalytic activity due to doping the Pd cluster with a Au atom.[6] Nakajima *et al.* reported the anion photoelectron spectroscopic studies of Pd, Ni, Zn, Cu, and Mg doped Au_n clusters,[7,8] providing electronic structure information on both the anion and neutral clusters.

Among these bimetallic clusters viewed as potential catalysts, the Pt-Al system is also an interesting candidate. In 1981, Worrell and Ramanarayanan reported that Pt_2Al and Pt_3Al alloys have special stability, which is because substantial bonding can be achieved with little electron configuration promotion.[9] Recently, Rees *et al.* found that Pt_3Al alloy used as fuel cell catalyst can facilitate the O_2 reduction catalysis.[10] Even though the above two studies focus on Pt-Al alloys and not small clusters, they nevertheless provide insight into this interesting bimetallic system. Additionally, Ouyang *et al.* performed a first principle theoretical study of PtAl dimer, identified its $^2\sum^+$ ground state, and calculated values of its bond length, vibrational frequency, and dissociation energy.[11] In the present work, we report a combined theoretical and anion photoelectron spectroscopic study of $PtAl^-$ and $PtAl_2^-$ dimer and trimer anions. Experimental and theoretical results are compared and utilized to characterize the electronic structures of both of these species.

METHODS

Experimental

The present work utilizes negative ion photoelectron spectroscopy as its primary probe. Anion photoelectron spectroscopy is conducted by crossing a mass-selected beam of negative ions with a fixed-energy photon beam and energy analyzing the resulting photodetached electrons. This technique is governed by the energy-conservation relationship, $h\nu$ = EBE + EKE, where $h\nu$, EBE, and EKE are the photon energy, electron binding (transition) energy, and the electron kinetic energy, respectively. Our photoelectron spectrometer, which has been described previously,[12] consists of one of several ion sources, a linear time-of-flight mass spectrometer, a mass gate, a momentum decelerator, a neodymium-doped yttrium aluminum garnet (Nd:YAG) laser for photodetachment, and a magnetic bottle electron energy analyzer. Photoelectron spectra were calibrated against the well-known photoelectron spectrum of Cu^-.[13] The $PtAl_{1,2}^-$ anions were generated using a pulsed arc cluster ionization source (PACIS), which has been described in detail elsewhere.[14] In brief, a ~30 μs long 150 V electrical pulse applied across anode and sample cathode in the discharging chamber vaporizes the Pt and Al atoms. The sample cathode was prepared in a nitrogen

a)Electronic addresses: kbowen@jhu.edu, Telephone: 001-410-516-8425 and ana@chem.ucla.edu, Telephone: 001-310-825-3769.

 © 2014 AIP Publishing LLC

This article is copyrighted as indicated in the article. Reuse of AIP content is subject to the terms at: http://scitation.aip.org/termsconditions. Downloaded to IP: 128.220.159.3 On: Wed, 30 Apr 2014 18:26:58

protected glove box, where fresh Pt and Al powders were mixed and firmly pressed onto an aluminum rod. About 150 psi of ultrahigh purity helium gas then propelled the Pt-Al plasma mix down in a 15 cm flow tube, where it reacted, formed clusters, and cooled. Anions generated by this method were then mass-selected prior to photoelectron spectroscopic studies.

Computational

Geometry optimization for the studied anions was carried out using the PBEPBE[15] and B3LYP[16] density functional theory (DFT) methods, as well as MP2.[17] LANL2DZ[18] and aug-cc-pvTZ-pp[19] basis sets were employed. Geometries obtained with different methods agree very well. Complete active space self-consistent field (CASSCF)(m,n)[20]/LANL2DZ single point energy calculations were also done to check whether or not the wavefunctions of the systems are single Slater determinants. The active space was chosen to be (6,6) for $PtAl^-$ and (5,6) for $PtAl_2^-$. For $PtAl^-$, the wavefunction was found to be primarily single-configuration, with the HF component contributing to the CASSCF expansion with the coefficient of 0.92. Therefore, single-reference methods are reliable for the diatomic anion. However, $PtAl_2^-$ was found to be more mixed, with the HF-configuration having a coefficient of 0.83 in the CASSCF expansion, and another configuration contributing most of the rest. Ideally, this cluster would require an extensive multi-reference treatment with static and dynamic electron correlation included. Unrestricted broken-symmetry DFT calculations are the most reliable in the present repertoire. The vertical electron detachment energy (VDE) is the energy difference between the optimized anion and the neutral with the anion structure. VDE was calculated using DFT and MP2 methods, as well as single point coupled-cluster single double triple (CCSD(T))[21]/aug-cc-pvTZ-pp level of theory. For the calculations of the other vertical transitions from the deeper valence molecular orbitals (MOs), time-dependent DFT calculations were performed to identify the excited states of the neutral species, which were then added to the VDE of the anion. For the doublet $PtAl_2^-$, electron detachments resulting in both the singlet and triplet states were calculated. The excited states of the anions were calculated using TD-PBEPBE and TD-B3LYP, with the aug-cc-pvTZ-pp basis set. MOs were obtained at the HF/aug-cc-pvTZ-pp level, and their order was chosen in agreement with the calculated transitions. Calculations were done using Gaussian 09.[22]

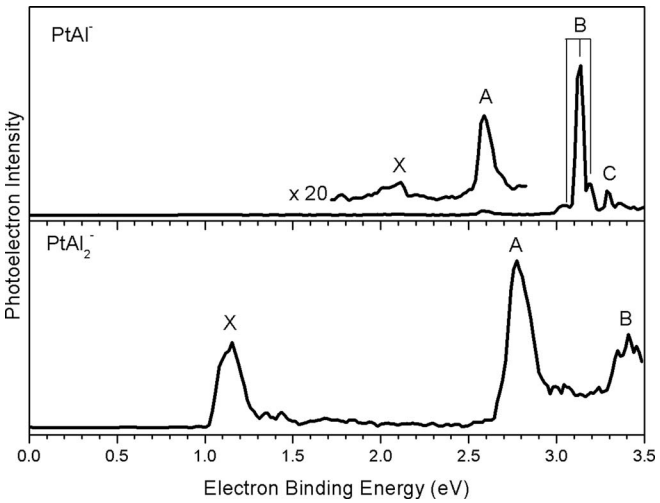

FIG. 1. Photoelectron spectra of $PtAl_n^-$ ($n = 1, 2$) recorded using 355 nm (3.49 eV) photons.

RESULTS AND DISCUSSION

Photoelectron spectra

The resulting photoelectron spectra of $PtAl_{1,2}^-$ are presented in Figure 1. In each spectrum, one can observe several peaks, these corresponding to transitions (photodetachment) from the ground state of the anion to different states of its corresponding neutral. For $PtAl^-$, we observe several peaks centered at 2.1, 2.6, 3.15, 3.3 eV, while for $PtAl_2^-$, these peaks are located at 1.1, 2.8, 3.4 eV. The lowest EBE peak in each spectrum is the VDE while the other peaks correspond to the photodetachment from deeper MOs of the anion. All of these experimental values are tabulated in Tables I and II.

Structures

The geometry and spin state of the $PtAl^-$ anion were obtained at various levels of theory. It is a singlet, and the optimized triplet and quintet are at least 1.5 eV higher in energy. The bond length values, R(Pt-Al) = 2.24/2.24/2.19 Å (at B3LYP, PBE, and MP2 levels, respectively) in the singlet state, are in good agreement with an existing study.[9] For the $PtAl_2^-$ anion, three geometries were considered: a triangular C_{2v} structure, and two linear ones, Pt-Al-Al$^-$ and Al-Pt-Al$^-$. The Al-Pt-Al$^-$ one is not a minimum. The spin state that allows the retention of the symmetry of this cluster is a quartet ($D_{\infty h}$, $^4\Sigma_g+$), which is a second-order saddle point. The normal mode of its doubly degenerate imaginary frequency leads

TABLE I. Calculated VDEs of $PtAl^-$ in eV comparing with those from the experiments. For the calculations, the aug-cc-pvTZ-pp basis set was used throughout. VDEs were calculated for structures optimized at the same level of theory unless stated otherwise.

Feature	Expt.	MO	Resultant e-configuration	TD-B3LYP	TD-PBEPBE	MP2	CCSD(T)
X	2.1	HOMO	$\ldots 1\sigma^2 1\pi^4 2\sigma^2 1\delta^4 3\sigma^1$	1.88	1.98	1.95	2.06[a]
A	2.6	HOMO-1	$\ldots 1\sigma^2 1\pi^4 2\sigma^2 1\delta^3 3\sigma^2$	2.46	2.43		
B	3.15	HOMO-2	$\ldots 1\sigma^2 1\pi^4 2\sigma^1 1\delta^4 3\sigma^2$	3.04	3.11		
C	3.3	HOMO-3	$\ldots 1\sigma^2 1\pi^3 2\sigma^2 1\delta^4 3\sigma^2$	3.20	3.30		

[a]At the geometry of the anion optimized using MP2/aug-cc-pvTZ-pp.

This article is copyrighted as indicated in the article. Reuse of AIP content is subject to the terms at: http://scitation.aip.org/termsconditions. Downloaded to IP: 128.220.159.3 On: Wed, 30 Apr 2014 18:26:58

TABLE II. Calculated VDEs of $PtAl_2^-$ in eV comparing with those from the experiments. (For the calculations, the aug-cc-pvTZ-pp basis set was used throughout.) VDEs were calculated for structures optimized at the same level of theory unless stated otherwise.

Feature	Expt.	MO	Resultant e-configuration	TD-B3LYP	TD-PBEPBE	MP2	CCSD(T)
X	1.1	HOMO	$\ldots 2a_1^2 1a_2^2 3a_1^2 2b_2^2 4a_1^2 2b_1^0$	1.02	1.12	0.96	1.01[a]
A	2.8	HOMO-1	$\ldots 2a_1^2 1a_2^2 3a_1^2 2b_2^2 4a_1^1 2b_1^1$[b]	2.64	2.69	2.73	2.73[a]
B	3.4		$\ldots 2a_1^2 1a_2^2 3a_1^2 2b_2^1 4a_1^2 2b_1^1$[b]	3.31	3.41		
C			$\ldots 2a_1^2 1a_2^2 3a_1^1 2b_2^2 4a_1^2 2b_1^1$[b]	3.72	3.75		
			$\ldots 2a_1^2 1a_2^1 3a_1^2 2b_2^2 4a_1^2 2b_1^1$[b]	3.98	4.04		

[a]At the geometry of the anion optimized using MP2/aug-cc-pvTZ-pp.
[b]Triplet state.

to the C_{2v} species. The linear Al-Al-Pt$^-$ species ($C_{\infty v}$, $^4\Sigma^+$), is a minimum with the energy ~2.2 eV higher than the global minimum. In it, R(Pt-Al) = 2.22 Å, R(Al-Al) = 2.48 Å. The triangular species is the global minimum in its doublet spin state (C_{2v}, $^2B_1$); R(Pt-Al) = 2.32/2.31/2.28 Å, ∠(Al-Pt-Al) = 71.53°/74.47°/75.29° (at PBE, B3LYP, and MP2, respectively). The quartet is ~1.4 eV above the doublet global minimum. The bent structure was also attempted, but relaxes to the triangular structure.

Calculated spectra

Calculated VDE and other transitions at different levels of theory are shown in Tables I and II. The agreement with the experiment and across the utilized theoretical methods is good, and all experimental features are successfully assigned to one-electron transitions from the ground state of the anions.

For $PtAl^-$ ($C_{\infty v}$, $^1\Sigma^+$), the ground state valence electronic configuration is $[core]1\sigma^2 1\pi^4 2\sigma^2 1\delta^4 3\sigma^2$. The valence MOs are shown in Figure 2(a). The theoretical spectrum appears to have the VDE of ~1.9 eV, which corresponds to the electron detachment from the HOMO (3σ). It is a very low-intensity peak in the experimental spectrum. All deeper transitions are perfectly described by the detachment of electrons from the valence MOs of the cluster. The experimental feature (marked by B) centered at 3.15 eV shows a resolved vibronic progression of ~620 cm^{-1} and ~480 cm^{-1}, and the error, 140 cm^{-1} is within the range of our apparatus' resolution. This vibronic progression makes sense, since the HOMO-2 ($2\sigma^+$) is a strongly bonding σ-MO between Pt and Al. Removal of an electron from this MO should result in a significant change in the vibrational frequency of the neutral cluster as compared to that of the anion. We did not pursue the calculations of the vibrational frequency of this excited state of the neutral cluster. The ground state of the neutral clusters has the calculated harmonic vibrational frequency of 397 cm^{-1}.

The $PtAl_2^-$ (C_{2v}, $^2B_1$) cluster has the following valence electronic configuration: $[core]1a_1^2 1b_2^2 1b_1^2 2a_1^2 1a_2^2 3a_1^2 2b_2^2 4a_1^2 2b_1^1$. Electron detachment from the doublet can result in the singlet and triplet final states. All transitions corresponding to the formation of triplet states are calculated and reported in Table II. The lowest energy detachment to the singlet state results from the removal of an electron from the HOMO of the doublet, and the corresponding VDE of ~1.1 eV is easily calculated. However, when the detachment happens from deeper MOs, the resultant singlet states are diradical, i.e., having wavefunctions that contain at least a two or potentially more (since the anion is multi-reference) configurations. These species cannot be adequately described with single-reference methods, even in the unrestricted DFT formalism. Therefore, we do not report those detachment energies, and only the first channel resulting in the singlet neutral cluster is reported in Table II. The assignment of the experimental peaks is also consistent with this. The first peak, located at 1.1 eV, corresponds to the transition from the doublet anion to the singlet, ground state neutral, and the second and third peaks at 2.8 and 3.4 eV match very well with the transitions from the doublet anion to the triplet neutral, while some minor unassigned features in the experimental spectrum might be due to the singlet neutral resulting from deeper MOs' detachment.

Chemical bonding

Both $PtAl^-$ and $PtAl_2^-$ exhibit significant polarization. The extra electron resides on Pt, leaving the Al atom(s) more or less neutral and in their unperturbed ground state. The Pt

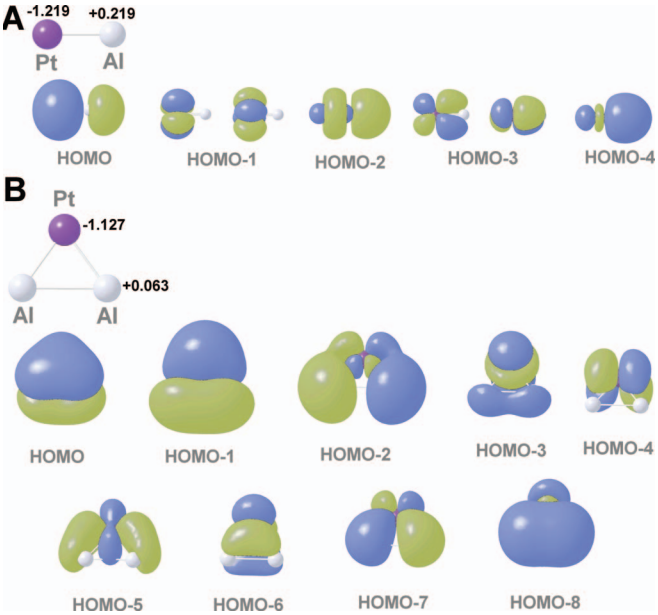

FIG. 2. Valence MOs of (a) $PtAl^-$ ($C_{\infty v}$, $^1\Sigma^+$), and (b) $PtAl_2^-$ (C_{2v}, $^2B_1$). Calculated atomic charges are also shown.

This article is copyrighted as indicated in the article. Reuse of AIP content is subject to the terms at: http://scitation.aip.org/termsconditions. Downloaded to IP: 128.220.159.3 On: Wed, 30 Apr 2014 18:26:58

atom in $PtAl^-$ has the 6s-AO populated with 1.52 electrons. In $PtAl_2^-$, there are 1.27 electrons in the 6s-AO and 0.25 electrons in the 6p-AO. Atomic charges and natural orbital populations were calculated using Natural Population Analysis[23] at the B3LYP/aug-cc-pvTZ-pp level. Charges are reported in Figure 2. The found charge distributions are in accordance with relative electronegativities of Pt and Al.

The analysis of valence MOs was used to realize how Pt and Al bind in these clusters. In $PtAl^-$ (Figure 2(a)), there are two σ-MOs formed mainly by the $5dz^2$-AO on Pt and the mix of 3s- and $3p_z$-AOs on Al, the HOMO-4, and HOMO-2. Since both the bonding and antibonding combinations are filled, the net-bonding effect of these MOs is nearly zero. Then, there is a degenerate pair of π-MO, the HOMO-3, formed by the $5d_{xz/yz}$-AO on Pt and $3p_{x/y}$-AO on Al. Both MOs are bonding. Finally, the HOMO of the cluster is a bonding MO that involves the 6s-AO on Pt (newly populated due to charge transfer to it) and the $3sp_z$-hybrid on Al. Thus, the formal bond order between Pt and Al in this cluster could be considered equal 3: there is a σ-bond, and 2 π-bonds.

The bonding in the $PtAl_2^-$ cluster is delocalized and more complicated (Figure 2(b)). The HOMO-1,2,3,5,7,8 are σ-MOs. Notice that 3s- and 3p-AOs on Al, and 6s- and four different kinds of 5d-AOs on Pt contribute to these MOs, as allowed by symmetry. The simplest linear combination of these seven AOs should produce the total of seven (bonding and antibonding) MOs. Only six of them are present in the valence set of MOs. Therefore, there is a net-bonding effect coming from this σ-set. The HOMO, HOMO-4, and HOMO-6 are π-MOs. The AOs that mostly contribute to them are $3p_z$ on Al, and $5d_{xz}$, $5d_{yz}$, and 6p on Pt. Out of these four AOs, four orthogonal linear combinations (MOs) can be produced, and only three of those are populated. The most antibonding π-MO is unoccupied. This indicates that the cluster also possesses delocalized π-bonding.

CONCLUSIONS

The experimental photoelectron spectra of the $PtAl_{1,2}^-$ anions are reported. Experimental electron detachment features are fully described by theoretical calculations. All peaks in the spectrum correspond to one-electron transition from the ground state of the anions to different states of the corresponding neutral. For $PtAl^-$, the resultant neutral electron configuration are mainly doublets, while for $PtAl_2^-$, the resultant neutral electron configuration is a singlet from the HOMO photodetachment. Photodetachments from deeper MOs resulting in triplets were calculated, and they adequately describe experimental spectra, and those resulting in singlet diradicals were not calculated. It is possible that some minor unassigned features in the experimental spectrum are due to the transitions of the latter type. Chemical bonding in these species was also explicated, and showed a significant charge transfer to Al, as well as a mix of σ- and π-bonding.

ACKNOWLEDGMENTS

This material is based on work supported by the Air Force Office of Scientific Research (AFOSR) under Grant Nos., FA9550-11-1-0068 (K.H.B.) and 10029173-S3 (A.N.A.).

[1] S. Simson, A. Jentys, and J. A. Lercher, J. Phys. Chem. C **117**, 8161 (2013).
[2] N. S. Venkataramanan, A. Suvitha, H. Mizuseki, and Y. Kawazoe, Int. J. Quantum Chem. **113**, 1940 (2013).
[3] L. B. Ortiz-Soto, J. R. Monnier, and M. D. Amiridis, Catal. Lett. **107**, 13 (2006).
[4] J. Rossmeisl, G. S. Karlberg, T. Jaramillo, and J. K. Norskov, Faraday Discuss. **140**, 337 (2009).
[5] D. Çakır and O. Gülseren, J. Phys. Chem. C **116**, 5735 (2012).
[6] J. Zhang and A. N. Alexandrova, J. Phys. Chem. Lett. **4**, 2250 (2013).
[7] K. Koyasu, M. Mitsui, A. Nakajima, and K. Kaya, Chem. Phys. Lett. **358**, 224 (2002).
[8] K. Koyasu, Y. Naono, M. Akutsu, M. Mitsui, and A. Nakajima, Chem. Phys. Lett. **422**, 62 (2006).
[9] W. L. Worrell and T. A. Ramanarayanan, Chem. Metall.–Tribute Carl Wagner, Proc. Symp. 69 (1981).
[10] G. J. Rees, S. T. Orr, L. O. Barrett, J. M. Fisher, J. Houghton, G. H. Spikes, B. R. C. Theobald, D. Thompsett, M. E. Smithac, and J. V. Hanna, Phys. Chem. Chem. Phys. **15**, 17195 (2013).
[11] Y. Ouyang, J. Wang, Y. Hou, X. Zhong, Y. Du, and Y. Feng, J. Chem. Phys. **128**, 074305 (2008).
[12] M. Gerhards, O. C. Thomas, J. M. Nilles, W. J. Zheng, and K. H. Bowen, J. Chem. Phys. **116**, 10247 (2002).
[13] J. Ho, K. M. Ervin, and W. C. Lineberger, J. Chem. Phys. **93**, 6987 (1990).
[14] X. Li, A. Grubisic, S. T. Stokes, J. Cordes, G. F. Gantefoer, K. H. Bowen, B. Kiran, M. Willis, P. Jena, R. Burgert, and H. Schnoeckel, Science **315**, 356 (2007).
[15] J. P. Perdew, K. Burke, and M. Ernzerhof, Phys. Rev. Lett. **77**, 3865 (1996); **78**, 1396 (1997).
[16] R. G. Parr and W. Yang, *Density-Functional Theory of Atoms and Molecules* (Oxford University Press, Oxford, 1989); A. D. Becke, J. Chem. Phys. **98**, 5648 (1993); J. P. Perdew, J. A. Chevary, S. H. Vosko, K. A. Jackson, M. R. Pederson, D. J. Singh, and C. Fiolhais, Phys. Rev. B **46**, 6671 (1992).
[17] M. Head-Gordon, J. A. Pople, and M. J. Frisch, Chem. Phys. Lett. **153**, 503 (1988); M. J. Frisch, M. Head-Gordon, and J. A. Pople, *ibid.* **166**, 275 (1990); **166**, 281 (1990).
[18] P. J. Hay and W. R. Wadt, J. Chem. Phys. **82**, 270 (1985); W. R. Wadt and P. J. Hay, *ibid.* **82**, 284 (1985); P. J. Hay and W. R. Wadt, *ibid.* **82**, 299 (1985).
[19] K. A. Peterson and C. Puzzarini, Theor. Chem. Acc. **114**, 283 (2005).
[20] J. A. Pople, M. Head-Gordon, and K. J. A. Raghavachari, J. Chem. Phys. **87**, 5968 (1987); D. Hegarty and M. A. Robb, Mol. Phys. **38**, 1795 (1979); R. H. A. Eade and M. A. Robb, Chem. Phys. Lett. **83**, 362 (1981); H. B. Schlegel and M. Robb, Chem. Phys. Lett. **93**, 43 (1982); F. Bernardi, A. Bottini, J. J. W. McDougall, M. A. Robb, and H. B. Schlegel, Faraday Symp. Chem. Soc. **19**, 137 (1984); M. J. Frisch, I. N. Ragazos, M. A. Robb, and H. B. Schlegel, Chem. Phys. Lett. **189**, 524 (1992); N. Yamamoto, T. Vreven, M. A. Robb, M. J. Frisch, and H. B. Schlegel, *ibid.* **250**, 373 (1996).
[21] J. Cizek, Adv. Chem. Phys. **14**, 35 (1969); G. D. Purvis III and R. J. Bartlett, J. Chem. Phys. **76**, 1910 (1982); G. E. Scuseria, C. L. Janssen, and H. F. Schaefer III, *ibid.* **89**, 7382 (1988); G. E. Scuseria and H. F. Schaefer III, *ibid.* **90**, 3700 (1989).
[22] M. J. Frisch, G. W. Trucks, H. B. Schlegel *et al.*, Gaussian 09, Revision A.1, Gaussian, Inc., Wallingford, CT, 2009.
[23] J. E. Carpenter and F. Weinhold, J. Mol. Struct.: THEOCHEM **169**, 41 (1988); J. E. Carpenter, Ph.D. thesis, University of Wisconsin, 1987; J. P. Foster and F. Weinhold, J. Am. Chem. Soc. **102**, 7211 (1980); A. E. Reed and F. Weinhold, J. Chem. Phys. **78**, 4066 (1983); A. E. Reed, L. A. Curtiss, and F. Weinhold, Chem. Rev. **88**, 899 (1988).

This article is copyrighted as indicated in the article. Reuse of AIP content is subject to the terms at: http://scitation.aip.org/termsconditions. Downloaded to IP: 128.220.159.3 On: Wed, 30 Apr 2014 18:26:58